Journal of Structural Geology, Vol. 16, No. 1, pp. 85 to 96, 1994
Printed in Great Britain

0191-8141/94 $06.00 + 0.00

The use of fluid inclusions to constrain fault zone pressure, temperature and kinematic history: an example from the Alpi Apuane, Italy

MARGARET A. HODGKINS* and KEVIN G. STEWART

Department of Geology, University of North Carolina, Chapel Hill, NC 27599-3315, U.S.A.

(*Received* 27 *April* 1992; *accepted in revised form* 26 *February* 1993)

Abstract—The Alpi Apuane is a tectonic window that exposes ductilely deformed greenschist facies metaigneous and metasedimentary rocks beneath relatively unmetamorphosed, brittlely deformed sedimentary rocks of the Tuscan nappe. The brecciated fault zone, the 'window fault', separating the two tectonic units was originally described as a simple thrust fault, but has recently been interpreted to have been reactivated as a later extensional detachment. Although evidence for extensional faulting is seen above and below the window fault, the amount of extensional displacement along this fault is unclear.

Fluid inclusions from veins cementing the fault breccia were used to estimate the pressures and temperatures during the last fault movement. Minimum pressure estimates obtained from these inclusions range from 105 to 240 MPa. Pressure-corrected trapping temperatures for these fluids range from about 300 to 345°C. These pressures and temperatures indicate that the fault was last active at a depth of about 10 km, assuming a geothermal gradient at the time of 31°C km^{-1}. This rules out complete extensional unroofing of the Alpi Apuane by movement along the window fault.

Fluid salinities increase abruptly from the footwall into the fault zone. This pattern suggests that fluids rose from the footwall, entered the fault zone and were channeled within it, leaching salt from the overlying evaporite. The lack of quartz veins above the fault zone indicates that these fluids did not circulate into the overlying Tuscan nappe.

INTRODUCTION

THE purpose of this study is to use fluid inclusion analysis to constrain the depths at which a major fault zone in the Northern Apennines of Italy was active. The applications of fluid inclusions to specific structural and tectonic problems has only recently begun to be explored (e.g. Vrolijk 1987, Yonkee *et al.* 1989, Boullier *et al.* 1991, Foreman & Dunne 1991, Srivastava & Engelder 1991). The significant role fluids play in rock deformation opens up a variety of possibilities for fluid-inclusion research in the area of tectonics and structural geology. Overthrusting of water-rich sediments and rocks during plate collision and subduction involves the expulsion of enormous quantities of fluids, large amounts of which pass back up the thrust surface and are channeled through the fault zone (Hubbert & Rubey 1959, Fyfe & Kerrich 1985, Oliver 1986, Vrolijk 1987). By looking at fluid inclusions within syntectonic veins in the footwall and hanging wall of the Willard Thrust, Wyoming, Yonkee *et al.* (1989) devised a thermal model for the emplacement of thrust sheets. Vrolijk (1987) analyzed fluid inclusions within syntectonic veins of the Kodiak accretionary complex and developed a model for the fluid-migration history in covergent margins. Fluid inclusions have also been used as structural indicators by relating the geometry of fluid migration to time–space relationships between deformational events and regional metamorphism (e.g. de Alvarenga *et al.* 1990, Cathelineau *et al.* 1990, Boullier *et al.* 1991).

In this study, we look at the temperatures and pressures of fluids trapped within a fault zone in order to estimate the depth(s) at which the fault was active. The Alpi Apuane is one of the few tectonic windows in the Northern Apennines that exposes ductilely deformed greenschist facies metamorphic rocks beneath the relatively unmetamorphosed, brittlely deformed sediments of the Tuscan nappe (Fig. 1). The brecciated fault zone separating the metamorphic rocks from the overlying Tuscan nappe (the 'window fault') has been the object of intense study (Dallan Nardi & Nardi 1973, Federici & Raggi 1974, Carmignani & Giglia 1975, 1977, 1983, Cerrina Feroni *et al.* 1976, Carmignani *et al.* 1978, Dallan Nardi 1979, Kligfield 1979, Kligfield *et al.* 1981, 1986, Sani 1985, Abbate & Bruni 1989), but the exact nature of the fault has been enigmatic. The window fault was previously described as a simple overthrust which doubled the Tuscan sequence and induced metamorphism in the footwall (e.g. Saggini 1965, Baldacci *et al.* 1967, Boccaletti & Guazzone 1968, Carmignani *et al.* 1978, Kligfield 1979). However, it has also been noted that there is a gap in the metamorphic grade between the ductile rocks below the fault and the brittle rocks above (Carmignani *et al.* 1978, Reutter *et al.* 1983). This feature has been cited as evidence that the original thrust plane was subsequently reactivated as a normal fault (Van den Berg 1990). Carmignani & Kligfield (1990) also presented structural evidence for extension in the Alpi Apuane, including extensional shear zones in the footwall metamorphic rocks and listric normal faults in the hanging wall.

The question we want to address is how much extensional displacement has taken place along the window fault. Were the metamorphics brought up to the surface through continual, large-scale extensional unroofing

*Current address: Amoco Production Company, 501 Westlake Park Blvd, P.O. Box 3091, Houston, TX 77253, U.S.A.

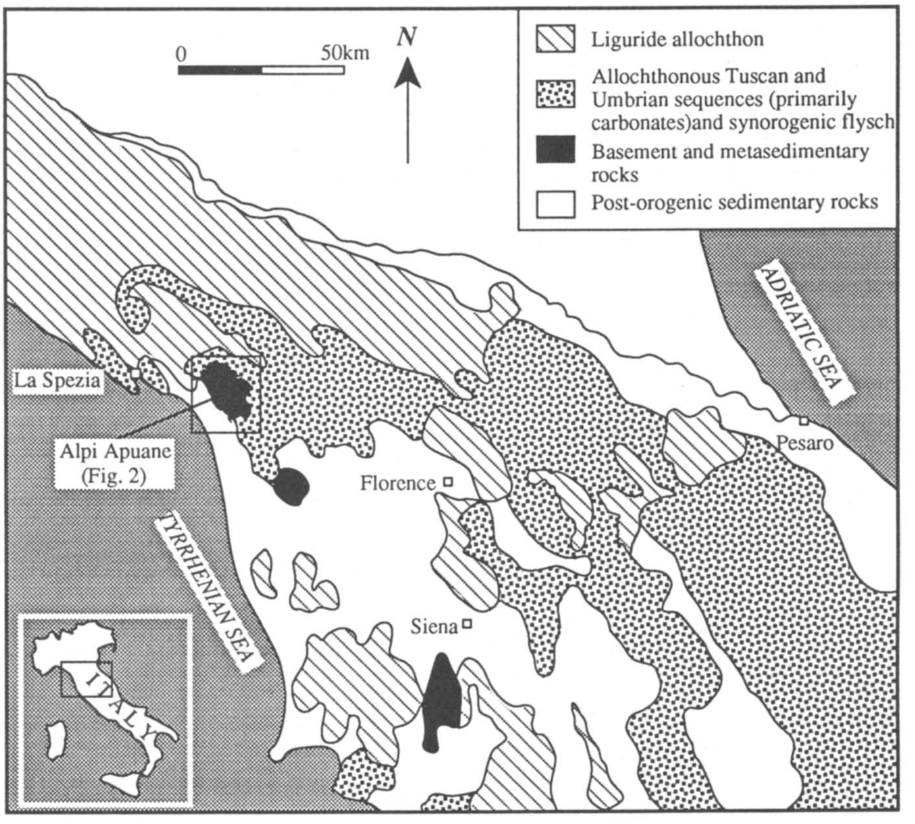

Fig. 1. Simplified geologic map of the Northern Apennines. The Liguride Allochthon (ancient accretionary wedge), together with the continental margin facies of the Tuscan and Umbrian sequences have been thrusted to the northeast. Basement and greenschist facies metasediments can be seen through three prominent windows, shown in black. The Alpi Apuane region is indicated.

along the window fault or was the fault only active at deep crustal levels and then later exhumed? A progressive overprinting of ductile structures by more brittle structures in the fault zone supports the idea that the fault was active at rising structural levels (Carmignani & Kligfield 1990), but the depths of faulting have not been quantified. In this study, we estimate the depth of the last faulting episode by measuring trapping temperatures and pressures of fluid inclusions within veins cementing the fault breccia. A similar technique was employed by Parry & Bruhn (1987) who estimated the vertical offset along the Wasatch fault by looking at fluid inclusions trapped within the fault rocks.

TECTONIC HISTORY AND CURRENT STRUCTURAL MODELS

In latest Cretaceous, as Africa began to converge on Europe, a W-dipping subduction zone developed on the eastern margin of the Corsica–Sardinia microplate, which was attached to the southern coast of France at the time (Treves 1984, Alvarez 1991). This plate apparently rotated away from the European plate towards the Adriatic plate consuming oceanic crust of the ancient Liguride Ocean in the process. The sediments deposited on the ocean floor were subducted and incorporated into an accretionary wedge (Treves 1984) and are now seen in allochthonous thrust sheets, collectively known as the Liguride Allochthon, over much of the Northern Apennines (Fig. 1). By Oligocene time, the Corsica–Sardinia plate had collided with Italy and thinned Italian continental crust and its sedimentary cover (the Tuscan sequence) began to be subducted (Kligfield 1979, Treves 1984). This collision thrust the Liguride allochthon over the Tuscan sequence, which was eventually detached, producing the Northern Apennine fold-and-thrust belt (Treves 1984, Bally *et al.* 1986). From Miocene time to the present, extension between Italy and the Corsica–Sardinia microplate has formed the Ligurian and Tyrrhenian Seas and has thinned the continental crust of western Italy to about 25 km (Elter *et al.* 1975, Malinverno & Ryan 1986). This extensional front has migrated from west to east across the Italian peninsula behind the migrating thrust front.

In the Tuscan Apennines, the tectono-stratigraphic sequences are, in ascending structural order: (1) Hercynian basement rocks and metamorphosed carbonates of the Tuscan sequence; (2) continental margin and carbonate platform rocks and flysch (Tuscan sequence); and (3) ophiolites and deep-water sediments of the Liguride sequences (Fig. 1). Studies of illite crystallinity and vitrinite reflectance show that the Tuscan and Liguride sequences are anchizonal, sub-greenschist facies (Venturelli & Frey 1977, Reutter *et al.* 1980, Cerrina Feroni *et al.* 1983). The Apuane metamorphic sequences within the window can be subdivided into three main units: (1) the basement rocks consisting of Paleozoic phyllites, quartzites and schists; (2) Mid- to Late-Triassic metasedimentary rocks (detrital sediments and volcanics) known as the Massa unit; and (3) Triassic to Oligocene metamorphosed carbonates and siliciclastics (marbles, dolomites, calcschists, phyllites, quartzites) equivalent to the Tuscan sequence (Carmignani *et al.* 1978, Kligfield 1979) (Fig. 2). Results from calcite–dolomite geothermometry (DiPisa *et al.* 1985) indicate a range of peak metamorphic temperatures from 460°C ± 40°C in the Massa unit of the western Alpi Apuane to 300°C ± 40°C in the eastern Alpi Apuane. These temperatures agree with mineral assemblages in the metamorphic rocks that are typical of chlorite and biotite zones of greenschist facies metamorphism (300–400°C and 300–400 MPa) (Giglia 1967, Franceschelli *et al.* 1986). Kligfield (1979) felt these temperatures and pressures were consistent with the idea that the metamorphism in the Alpi Apuane was induced by the overthrusting of a sedimentary cover 10–12 km thick. K–Ar and $^{40}Ar/^{39}Ar$ dating of phengitic white micas in slates and schists show multiple episodes of deformation, from 27 to 10 Ma, in the rocks inside the window (Kligfield *et al.* 1986). Carmignani & Kligfield (1990) attribute the earliest phase (D_1) to a compressional event and the later phase (D_2) to extension. They infer temperatures of 350–400°C for D_1 and a temperature of 350°C for D_2 based on cooling ages of syntectonic minerals in the footwall metamorphic rocks.

The window fault zone consists of breccias and cataclasites primarily made up of dolostone, dolomitic limestone fragments and metamorphic clasts from the footwall. Although some workers propose that sedimentary breccias are also found at this contact (Federici & Raggi 1974, Dallan Nardi 1979, Sani 1985, Abbate & Bruni 1989), we are restricing our study to a clearly tectonic breccia. This breccia corresponds to the part of the fault zone immediately above ductilely deformed metamorphic rocks and was generated by progressive fracturing of these footwall rocks. Fracturing becomes more intense higher in the fault zone and ultimately incorporates fragments of the hanging wall.

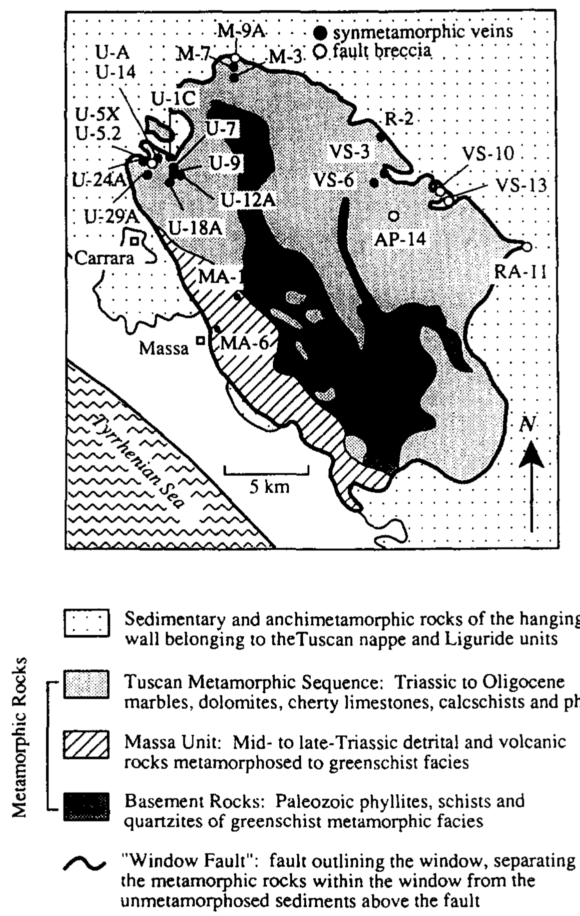

Fig. 2. Simplified geologic map of the Alpi Apuane with fluid inclusion sample locations.

STRATEGY FOR FLUID INCLUSION STUDY IN THE ALPI APUANE

We use fluid inclusions to estimate temperatures and pressures in the veins forming the matrix of the brecciated window fault zone. Fluid inclusions are samples of presumably homogeneous fluids trapped in minerals during crystal growth or healing of microfractures (Roedder 1984). Minimum fluid trapping temperatures are estimated by the temperature of homogenization of the liquid, vapor and solid phases within an inclusion to one fluid phase. The homogenization temperature of a fluid inclusion together with the fluid composition determines the density of an inclusion which is used to define a unique isochore (line of constant density) that represents the range of P–T conditions over which fluids of that density could have been trapped (Hollister 1981). Fluid inclusion data alone provide only a minimum estimate of the trapping temperature and pressure, but if either temperature or pressure are known independently, a higher trapping temperature and corresponding pressure can be determined from the isochore.

The pressures and temperatures obtained from the fluid inclusions can be used to estimate the depths at which the fault was active. If the window fault was active at shallow crustal levels as well as the deeper levels indicated by ductile extensional structures in the footwall rocks (Carmignani & Kligfield 1990), this would imply that unroofing of the window metamorphic rocks was accomplished by large extensional displacement along the window fault. On the other hand, if the fault was only active at relatively deep depths, this would indicate that the footwall metamorphic rocks were exhumed through erosional processes or extension accommodated by other faults.

SAMPLING AND ANALYTICAL TECHNIQUES

Fluid inclusion samples in the window fault breccia are from calcite and quartz veins cementing the breccia (Fig. 3a). Our samples come from the base of the fault zone and consist primarily of brecciated metamorphic rocks which correspond to the highest structural level within the footwall. The quartz and calcite veins cementing the fault breccia are assumed to be samples of syntectonic fluids that were channeled along the fault zone and trapped by the progressive cracking and sealing of fractures during fault movement. Seven samples were collected from the fault zone at widely spaced regions around the edge of the window (Fig. 2).

Samples from below the fault were taken from quartz veins located within 500 m of the window fault (Fig. 3b). Because no quartz veins are present in the nearby unmetamorphosed Tuscan sequence, the veins within the metamorphic rocks of the Alpi Apuane presumably formed during the Tertiary metamorphic and deformational event in the Northern Apennines. No retrograde metamorphic event has been recognized. The veins cut the D_1 foliation in calcareous schists, phyllites and quartzites of the footwall (Carmignani *et al.* 1978), and are likely to be associated with the later stages of metamorphism. These samples were compared with those within the fault zone in order to get an idea of the relative timing of faulting, metamorphism and fluid flow in the window. A total of 16 quartz veins were analyzed from within the window (Fig. 2).

Thermometric measurements of fluid inclusions were made with a Fluid, Inc., U.S. Geological Survey gas-flow heating–freezing stage. Measurements were made on doubly polished, unmounted 'thick' sections (100–200 μm thick) following methods described by Hollister (1981) and Roedder (1984). Observations were made on euhedral, well-formed inclusions, while irregular and necked inclusions were avoided. These inclusions include both isolated inclusions and those along trails or fractures. Groups of inclusions in a sample with similar sizes, phase ratios and thermometric characteristics are assumed to represent the same 'fluid event' or fluid trapping episode. Representative inclusions within such groups were measured and compared with other groups or individual inclusions within the sample to get an overall idea of the composition and trapping temperature of the fluid.

Minimum fluid trapping temperatures for aqueous inclusions are determined by the temperature of homogenization of the liquid and vapor phases into one fluid phase (T_h L–V). Trapping temperatures of aqueous fluids containing halite daughter minerals are based on the temperature and order of disappearance of the two phases, H_2O vapor and solid NaCl. It is assumed that the fluids were trapped as a single homogeneous phase because of the consistent size of the halite cubes relative to the total volume of the fluid inclusion. Since the solid halite dissolves after the H_2O-liquid-and-vapor homogenization for all of the halite-bearing fluids in this study, the halite dissolution temperature (T_m NaCl) provides a higher minimum value for fluid trapping temperatures. Fluid compositions and salinities were calculated by the melting point of ice for H_2O–NaCl inclusions (Hall *et al.* 1988), the CO_2 hydrate (clathrate) melting temperature for H_2O–CO_2–NaCl inclusions (Bozzo *et al.* 1975), and the halite melting temperature when halite daughter minerals were present (Bodnar *et al.* 1989). Fluid compositions and homogenization temperatures define the fluid densities which are then used to construct isochores that represent a range of pressures and temperatures at which the fluids must have been trapped (Roedder 1984). Fluid inclusion measurements only give minimum *P–T* conditions initially, but these measurements can be refined using isochores and an independent measure of either temperature or pressure.

Multiple measurements were made on each inclusion and temperatures were usually reproducible within ±1.0°C for liquid–vapor homogenization, ±0.2°C for ice melting, ±0.9°C for clathrate melting and ±4.5°C for halite dissolution. Heating measurements made on fluid inclusions in calcite were often repeated only once or twice in order to avoid stretching of the mineral walls, which leads to inaccurate homogenization temperatures. Halite melting temperatures were sometimes only measured once since the salt often does not re-nucleate on cooling, or if the disappearance of the daughter phase was clearly visible, which usually is true in larger inclusions.

FLUID INCLUSION RESULTS

Minimum fluid trapping temperatures

Fluid inclusions trapped in quartz and calcite veins cementing the fault breccia are all H_2O-rich fluids containing halite daughter minerals. They contain three phases at room temperature: solid NaCl, NaCl-saturated H_2O liquid and NaCl-saturated H_2O vapor (Fig. 3c). The fluids trapped in the fault zone must have had a sufficiently high NaCl concentration to precipitate solid daughter crystals of halite upon cooling. It is possible that other dissolved salts are present in the liquid and vapor phases (e.g. KCl), but in this study we will treat the salinities as NaCl-equivalents. The fault fluids show a range of minimum trapping temperatures from 240 to 330°C for all measured inclusions, based on halite dissolution temperatures (Fig. 4c). When these measurements are averaged for individual samples the range is 250–320°C (Table 1). Temperatures (T_h L–V and T_m NaCl) measured from inclusions occurring as individuals and along growth zones are similar to the temperature measurements made on inclusions along trails and fractures within the same samples, so no multiple fluid events seem to exist. Once the H_2O vapor and liquid phases homogenize into one fluid phase, the pressure within the halite-bearing inclusions increases rapidly with continued heating. This sometimes leads to decrepitation of the inclusion before halite dissolution occurs, especially in calcite. Since decrepitation usually occurs between T_h L–V and T_m NaCl, the decrepitation temperatures were occasionally used to estimate minimum trapping temperatures when destruction of the inclusion occurred before the phase change (e.g. sample U-5.2).

Most of the fluid inclusions within synmetamorphic veins of the footwall are H_2O rich, containing both a liquid and vapor phase at room temperature and homogenizing to the liquid phase upon heating (Fig. 3d). Two samples from the footwall, U-24A and M-7, con-

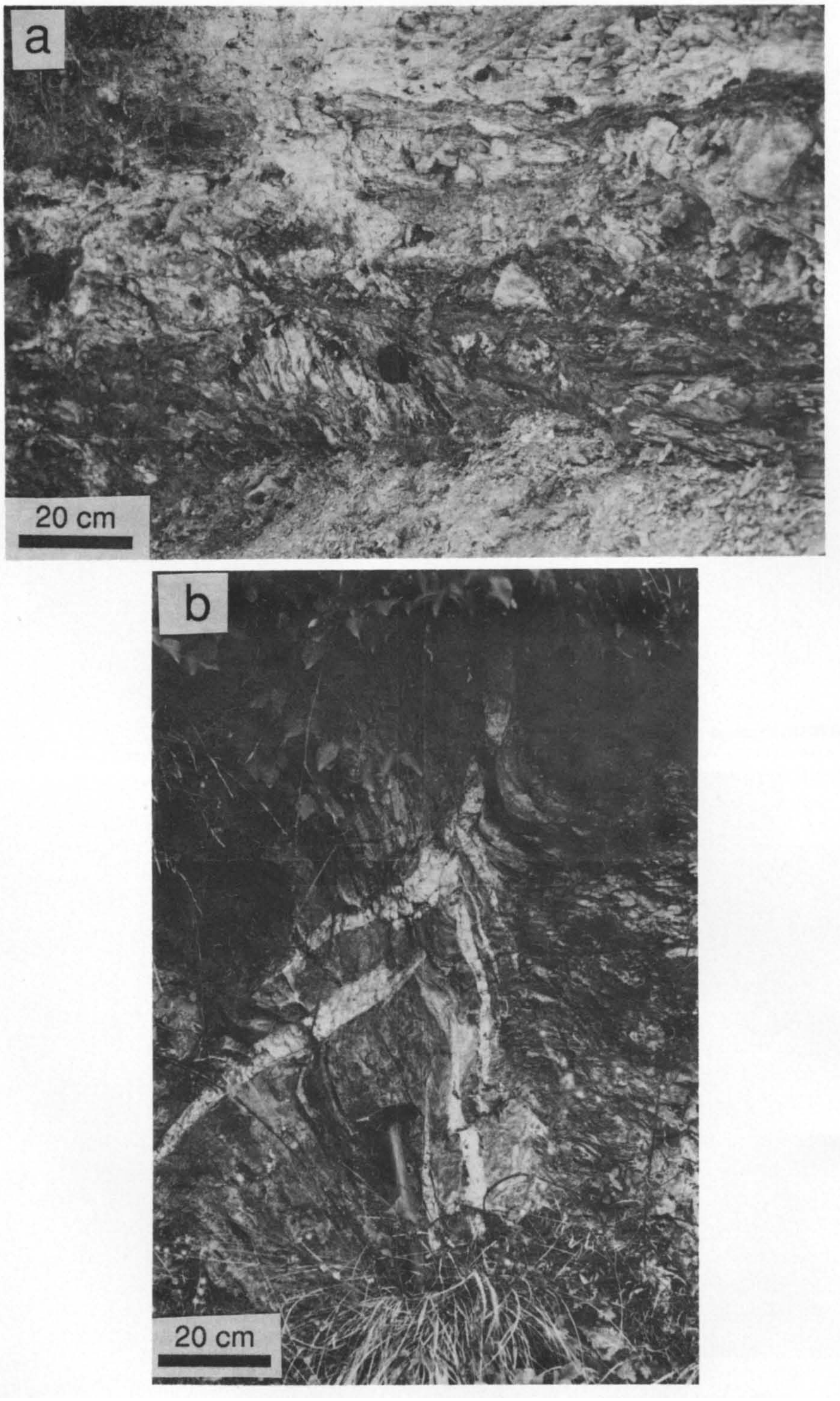

Fig. 3. (a) Photograph of the window fault breccia at the base of the Tuscan nappe. The fault zone is made up of brecciated limestones and dolostones in a cataclastic matrix, often containing metamorphic clasts from the footwall. The trace of the fault zone on the exposed face is roughly horizontal. Fluid inclusion samples in the fault zone were taken from quartz and calcite veins cementing the fault breccia. The photograph is from sample locality VS-10. (b) Photograph of synmetamorphic quartz vein. The vein is from sample locality VS-6, approximately 200 m below the window fault. The quartz vein is cutting foliation in the Calcare Selciferi.

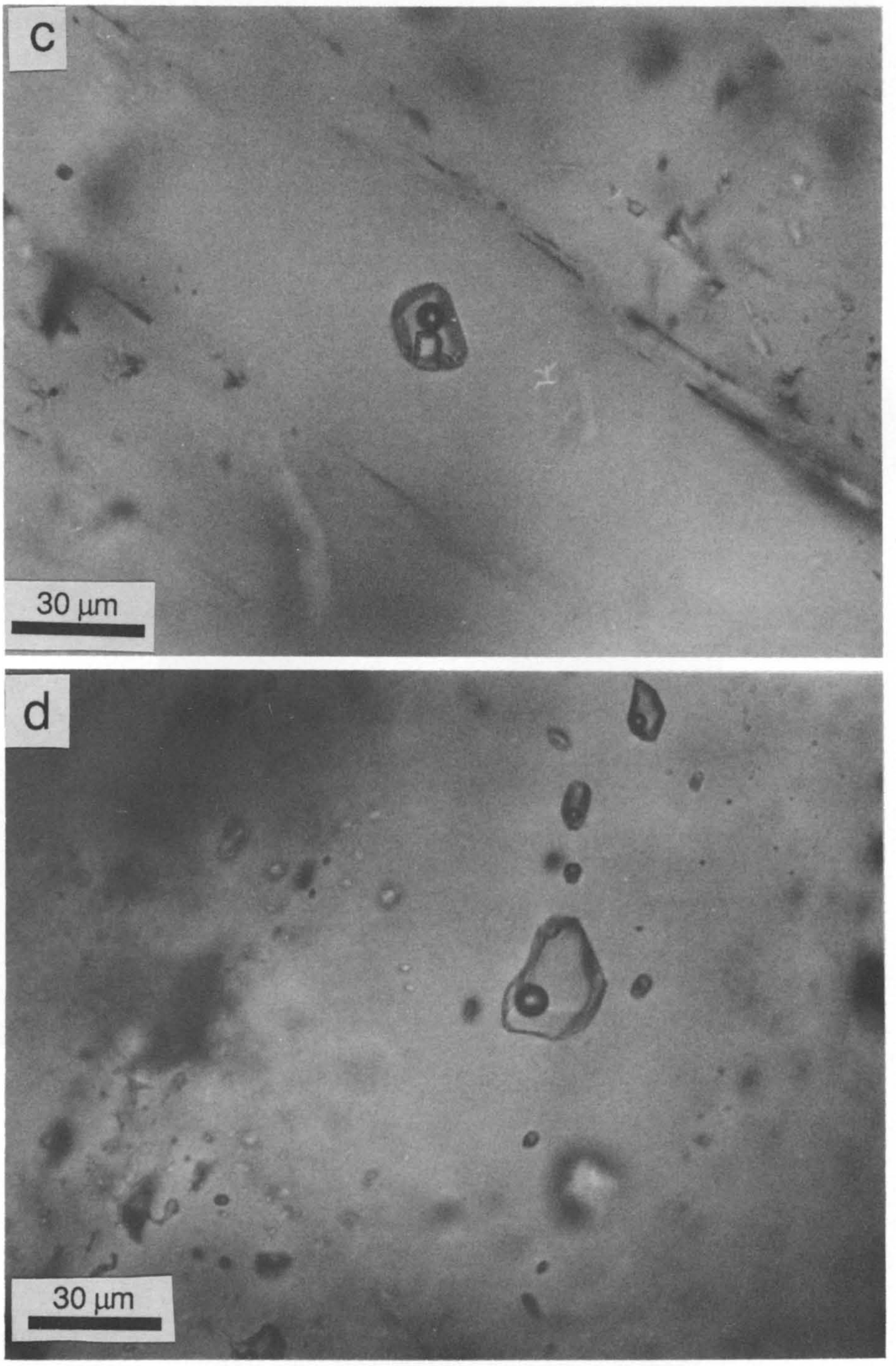

Fig. 3. (c) Photomicrograph of fluid inclusion from calcite vein within fault breccia. The inclusion contains three phases at room temperature: solid NaCl, NaCl-saturated H_2O liquid, and NaCl-saturated H_2O vapor. The photograph is of sample U-5.2. (d) Photomicrograph of fluid inclusions from synmetamorphic quartz vein. The fluid inclusion contains liquid H_2O with dissolved NaCl and H_2O vapor at room temperature. The photograph is of sample U-A.

Table 1. Summary of fluid inclusion data

		No. of inclusions or groups analyzed	T_h L–V (°C)	P-corr T°C (at 240 MPa)	P_{min} (MPa)	T_m NaCl (°C)	T_m Ice (°C)	Wt% NaCl	Density (g cm^{-3})	Distance from fault plane (m)
Synmetamorphic veins										
H_2O–NaCl	R-2	10	138.3 ± 5	271			−7.6 ± 1	11.1	1.007	*
	U-12A	11	216.0 ± 5	359			−10.7 ± 2.8	14.5	0.961	407
	U-14	6	147.0 ± 6	283			−3.8 ± .6	6.1	0.965	50
	U-18A	9	143.1 ± 9	276			−8.7 ± .5	12.5	1.014	486
	U-1C	11	209.8 ± 10	342			−21.9 ± 5.5	23.2	1.039	10
	U-29A	6	162.4 ± 15	300			−3.1 ± .5	4.9	0.943	110
	U-7.1	5	159.4 ± 5	289			−10.7 ± 1	14.6	1.016	336
	U-7.2	5	223.2 ± 12	367			−13.3 ± 1.3	17.1	0.973	336
	U-9	10	202.8 ± 9	343			−8.6 ± 1.3	12.4	0.958	480
	U-A	10	194.1 ± 7	336			−7.0 ± .2	10.4	0.951	32
	VS-3	5	173.2 ± 12	312			−3.3 ± .7	5.3	0.935	57
	VS-6	9	159.1 ± 6	296			−4.2 ± .6	6.6	0.957	216
H_2O–CO_2–NaCl	M-3	8	167.5 ± 8	*				3.8	*	*
	MA-1	10	270.5 ± 8	*				5.8	*	*
	MA-6	6	236.4 ± 6	*				6.5	*	*
H_2O–NaCl (with halite)	M-7	10	173.1 ± 7	301	170	263.4 ± 13		35.6	1.17	38
	U-24A.1	2	168.6 ± 12	295	152	247.3 ± 2		34.5	1.165	17
	U-24A.2	10	217.1 ± 13	371	124	302.1 ± 25		38.4	1.153	17
Fault breccias										
H_2O–NaCl (with halite)	AP-14	7	183.6 ± 8	328	223	319.5 ± 10		39.7	1.195	0
	M-9A	6	166.2 ± 12	300	240	305.0 ± 12		38.9	1.203	0
	RA-11	10	183.6 ± 3	326	203	306.0 ± 8		38.7	1.185	0
	U-5X	4	200.2 ± 9	337	105	263.7 ± 15		35.6	1.145	0
	VS-10	8	169.3 ± 4	299	185	269.6 ± 7		36	1.176	0
	VS-13	8	171.5 ± 6	299	155	252.5 ± 8		34.8	1.165	0
	U-5.2	5	199.5 ± 7	345	165	302.0 ± 8		38.3	1.168	0

Values given are averages for all inclusions measured in a given sample ± 1 standard deviation.
*Insufficient data to calculate.

tain inclusions with halite daughter minerals indicating a NaCl-saturated aqueous solution at room temperature. These samples are both located within 30 m of the fault zone. Three samples from the footwall (MA-1, MA-6, M-3) contain mixed H_2O–CO_2–NaCl fluid inclusions. These inclusions contain two visible phases (liquid H_2O+CO_2–H_2O vapor) at room temperature and totally homogenize to the liquid H_2O phase. No liquid CO_2 rim is visible at or above room temperature, indicating that the CO_2 content is much less than 100 mole% (Touret 1977, Hendel & Hollister 1981, Bodnar 1983). The melting temperature of solid CO_2 at approximately −56.6°C indicates the absence of significant amounts of other gases.

In the fluid inclusions from the footwall veins, 90% of the samples show liquid–vapor homogenization temperatures between 140 and 250°C (Fig. 4a). The two samples with halite-bearing fluids show higher minimum trapping temperatures of ~250–300°C since these temperatures are based on halite dissolution rather than liquid–vapor homogenization (Fig. 4b). Two samples from the Massa unit in the western part of the Alpi Apuane both contain H_2O–CO_2–NaCl fluids and show noticeably higher bulk homogenization temperatures of ~235–270°C which is consistent with the fact that the metamorphic grade in the Alpi Apuane is greater in the western part of the window than in the central or eastern zones, as mentioned earlier (DiPisa *et al.* 1985). Measurements of inclusions within a given sample are relatively consistent, indicating a single fluid event. The only exceptions to this are in samples U-24A and U-7, which each contain fluids that show two distinct temperature ranges, both of which still fall within the overall range of temperatures for the footwall fluids (Table 1).

A potential problem encountered in fluid inclusion studies in metamorphic terranes is that varying metamorphic pressures may permanently alter the volume of the fluid inclusions, thereby changing the density of the trapped fluid (Sterner & Bodnar 1989). This is mainly a problem for fluid inclusions formed during the early stages of regional metamorphism or for inclusions in soft minerals such as calcite, and it usually produces a large scatter in calculated fluid densities. In this study, fluid inclusions measured are from veins formed during the later stages of metamorphism and the calculated fluid densities are consistent within a given sample as well as between samples, whether in quartz or calcite. We believe this is sufficient evidence to infer that the calculated densities of the measured fluid inclusions are representative of the fluid densities at the time of trapping.

Salinities and densities

Salinities for the aqueous fluids are estimated from the ice melting temperatures (T_m Ice). A weight percentage of equivalent NaCl was determined for each sample, using averaged measurements of T_m Ice for individual inclusions and data from Hall *et al.* (1988) (Table 1). Sample averages of salinity are then used to determine sample fluid densities using data from Haas (1976). Salinities of halite-bearing fluids are based on halite dissolution temperatures (T_m NaCl). The average T_m NaCl for a given sample is used in the Fortran program *SALTY* (Bodnar *et al.* 1989) to determine the fluid salinity. The density of halite-bearing inclusions is calculated using the salinity and the procedures described by Roedder & Bodnar (1980).

The halite-bearing fault fluids give average halite dissolution temperatures of ~250–320°C (Table 1). These temperatures define salinities in the range of 35–40 wt% NaCl (Fig. 5) and densities in the range 1.145–1.203 g cm^{-3} for the fault fluids. Aqueous fluids in the synmetamorphic veins of the footwall give ice melting temperatures in the range of −22 to −3°C (Table 1), indicating salinities in the range of 4–23 wt% NaCl for these fluids (Fig. 5). Most of these samples fall in the range 4–17 wt% NaCl, however the sample U-1C, a quartz vein cutting a schist unit within 10 m of the fault zone, has an average T_m Ice of −21.9°C corresponding to ~23 wt% NaCl. Halite-bearing fluids in samples from footwall veins give salinities of 35–38 wt% NaCl based on halite dissolution temperatures in the range of 250–300°C. The three footwall samples containing H_2O–CO_2–NaCl fluids show clathrate melting temperatures of 6.5 – 8°C (Table 1) corresponding to 3.8–6.5 wt % NaCl (Fig. 5). Densities of fluids within the footwall veins show a range from 0.935 to 1.170 g cm^{-3} with the higher values (1.1 g cm^{-3}) corresponding to halite-bearing fluids. The density estimation for the CO_2-bearing fluids, using sample MA-1, is 0.780 g cm^{-3}.

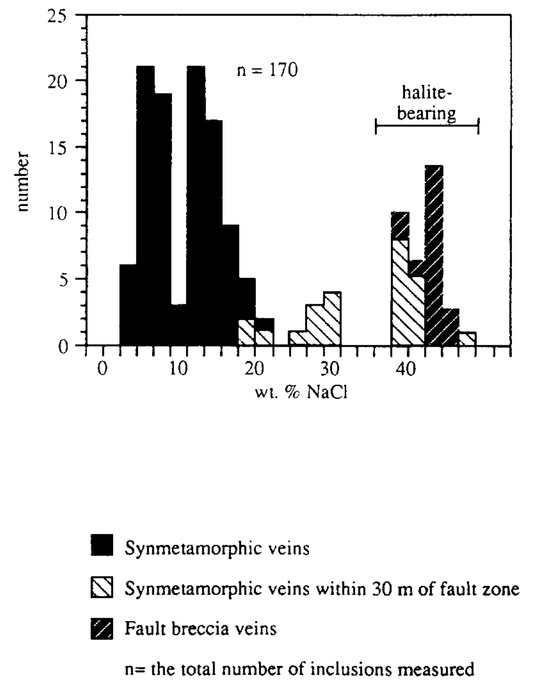

Fig. 5. Salinities of fluids in the synmetamorphic veins and fault breccia based on T_m Ice (fluid composition = H_2O+NaCl), T_m Clath (fluid composition = H_2O+CO_2+NaCl) and T_m NaCl (fluid composition = H_2O+NaCl with halite). Measurements are for individual inclusions in each sample.

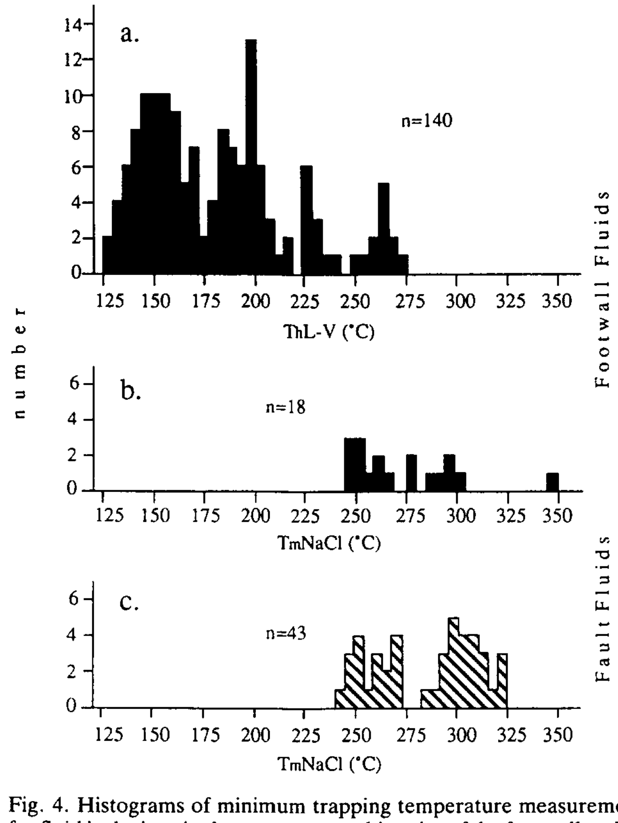

Fig. 4. Histograms of minimum trapping temperature measurements for fluid inclusions in the synmetamorphic veins of the footwall and the fault breccia. (a) Trapping temperatures for aqueous fluids in synmetamorphic veins are based on the homogenization of the H_2O liquid and vapor phases to one liquid phase (T_h L–V) and (b) on halite dissolution temperatures (T_m NaCl) for fluid inclusions containing halite. (c) Fault fluids all contain halite and the trapping temperatures are all based on T_m NaCl. n = number of inclusions measured in each case.

Fluid isochores and corrected temperatures

Isochores have been constructed for fluids within the fault breccia and synmetamorphic veins of the footwall. The isochores for aqueous fluids (H_2O–NaCl) are constructed using sample averages of salinity and homogenization temperature together with the equation of state from Brown & Lamb (1989) and the computer program *FLINCOR* (Brown 1989). For halite-bearing aqueous fluids, sample averages of density, salinity, and halite dissolution temperature are used with P–V–T data from Bodnar & Sterner (1985) to generate isochores. Once all of the isochores are constructed, two isochore 'envelopes' are drawn: one includes all calculated isochores for fluids in the fault breccia and the other includes all calculated isochores for fluids in the synmetamorphic veins of the footwall (Fig. 6).

The minimum trapping pressure of a homogeneous fluid at the homogenization temperature is obtained from the calculated isochore for each fault breccia sample. Minimum fluid pressures range from 105 to 240 MPa in the fault zone (Fig. 7). The 240 MPa pressure corresponds to a temperature of 305°C, consistent with a 31°C km^{-1} thermal gradient. Using this thermal gradient and methods employed by Parry & Bruhn (1987), we calculated that this pressure is equal to lithostatic pressure at a depth of 10 km. The thermal gradient could be lower, leading to greater estimated depths, but if the gradient is more than 31°C km^{-1}, fluid trapping pressures would be higher than lithostatic pressures. Figure 7 shows that for a given depth, fluid trapping pressures vary between hydrostatic and lithostatic conditions. In addition, minimum trapping pressures for all fault breccia samples correspond to depths from about 8 to 10.5 km.

Temperature estimates for fluids in the fault zone and metamorphic rocks can be corrected by estimating the lithostatic load above the fault. Minimum fluid trapping temperatures in the fault breccia range from 250 to 320°C (Table 1). Fluids in the synmetamorphic veins directly below the fault were presumably trapped during the later stages of metamorphism since these veins cut D_1 foliations in the metamorphic rocks. Carmignani & Kligfield (1990) ascribe a temperature of about 350°C to these later events. The similarity in temperatures shows that the fault zone and uppermost part of the footwall were at about the same crustal level during the trapping of these two fluids. Therefore, the lithostatic load once present above the fault zone and the underlying metamorphic rocks is presumed to be the same and can be used to correct minimum trapping temperatures of these two fluids.

The sedimentary load once above the Alpi Apuane most likely consisted of Tuscan and Liguride units that currently outcrop outside the window (Abbate & Sagri 1970, Bortolotti *et al.* 1970). The total thickness of these units ranges from about 10 to 17 km, which corresponds to lithostatic pressures of 240–408 MPa, assuming an average rock density of 2.45 g cm^{-3} for limestone and sandstone. These values agree with Kligfield's (1979) estimates of a 10–12 km sedimentary cover necessary for the 300–400 °C and 300–400 MPa metamorphic rocks in the Alpi Apuane. We use the minimum estimates for

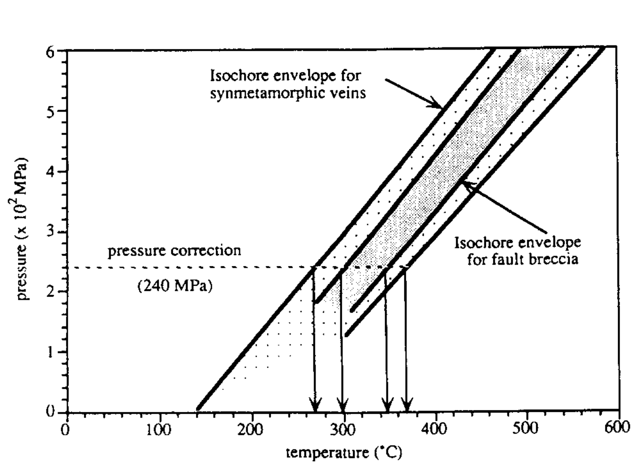

Fig. 6. Isochore envelopes that include all calculated isochores for fluids in the fault breccia and synmetamorphic veins of the footwall. Isochores were generated using sample averages of minimum trapping temperatures and densities. A pressure-correction of 240 MPa was used assuming a 10 km lithostatic load above the fault zone. Pressure-corrected minimum trapping temperatures range from 271 to 371°C for the synmetamorphic fluids and from 299 to 345°C for the fault fluids.

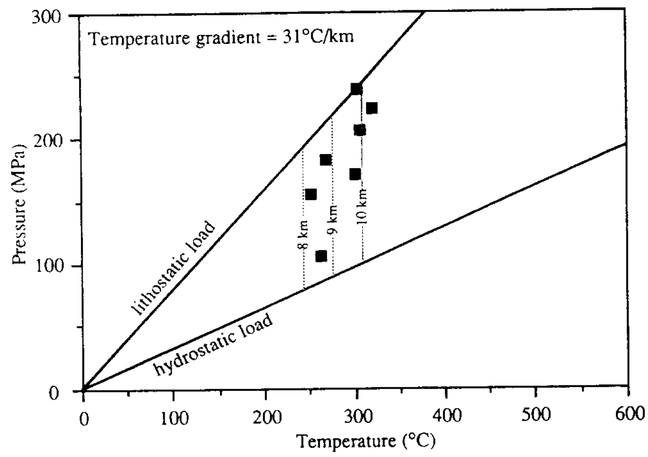

Fig. 7. Fluid pressures and temperatures for fluid inclusions in the window fault breccia. Lithostatic and hydrostatic pressure gradients are for densities of 2.45 and 1.0 g cm^{-3}, respectively, and are based on a thermal gradient of 31°C km^{-1}.

lithostatic overburden of 10 km and 240 MPa pressure to correct the minimum trapping temperatures for the fault and footwall fluids to higher minimums along isochores (Fig. 6).

Fluids within the fault breccia have corrected minimum trapping temperatures in the range of 299–345°C while the fluids in the footwall veins show a wider range of corrected trapping temperatures from 271 to 371°C (Fig. 6). These corrected temperatures for the footwall fluids are comparable with the estimates for peak metamorphic temperatures of 300–460°C±40°C, derived from calcite–dolomite thermometry (DiPisa *et al.* 1985), and with the estimated temperatures of 300–400°C necessary for greenschist facies metamorphism in the window (Carmignani *et al.* 1978).

DISCUSSION AND CONCLUSIONS

Carmignani & Kligfield (1990) have strong evidence, based on the growth of synkinematic mineral phases, that late-stage extension occurred at mid-crustal levels (350°C) within the Alpi Apuane. These temperature estimates correspond to ductile extensional shear zones within the metamorphic rocks. Given that the ductile extensional structures have been overprinted by brittle structures in the window fault zone, we know that faulting along this detachment occurred at progressively shallower depths in the crust, but the exact depths have not been quantified. Our goal is to constrain the minimum depths at which extension along the window fault occurred by looking at the *P–T* conditions of the fluids circulating through the fault zone during faulting.

Estimating the displacement on the window fault is difficult because there are no recognizable offset markers. A rough estimate of the displacement can be made if we assume that, for a given dip of the fault plane, the greater the range of depths at which the fault was active, the greater the displacement along the fault. If the window fault had been continuously active as it was progressively uplifted from middle to shallow crustal depths, this would imply that the fault had a relatively large displacement. In such a case, it is likely that unroofing of the Alpi Apuane metamorphics occurred primarily by large-scale extension along the window fault (Fig. 8). On the other hand, if the window fault was only active while at mid-crustal levels, uplift of the fault surface and unroofing of the metamorphic rocks would have occurred primarily by erosion or by extensional faulting along other detachments (Fig. 8).

Using a thermal gradient of 31°C km^{-1}, calculated fluid pressures in the fault zone give a range of minimum depths of faulting from 8.2 to 10.4 km. This range might reflect faulting at progressively shallower levels, but since these are only minimum depth estimates, we can only say that the window fault was not active at depths less than 8.2 km. The range in fluid pressures for a given temperature may be a result of pressure fluctuations caused by cracking and sealing of fluid conduits. Pressure-corrected temperatures for fluids in the fault breccia range from about 300 to 345°C, indicating that the last fault movement occurred at temperatures similar to those of metamorphism in the window. Therefore, it appears that movement along the window fault occurred only at mid-crustal or slightly shallower levels, coeval with the later stages of metamorphism. A significant amount of the unroofing of the Alpi Apuane metamorphic rocks must have occurred by erosion or extension along other detachments (Fig. 8).

Fluid salinities and the implications for fluid flow

In the Alpi Apuane, the major and most obvious source of water during low-grade regional metamorphism is the physical expulsion of interstitial pore water from the compaction of sediments during subduction and thrust faulting. Other volatiles, including water, are expelled in lesser amounts by chemical devolatilization induced by metamorphic reactions (Etheridge *et al.* 1983, Roedder 1984). It may also be possible to have meteoric water and/or other fluids percolating down through the hanging wall, eventually reaching the fault zone and becoming channeled within it.

Fluid salinities are consistently high (>23 wt% NaCl) within 50 m of the fault zone, but drop off abruptly at distances greater than 50 m from the fault and remain fairly uniform (5–15 wt% NaCl) down to 500 m below the fault (Fig. 9). The abrupt drop in salinity seems to show that fluids rising from the footwall enter the fault zone and are channeled within it, becoming saturated with salt from the evaporite above, but do not recirculate to any significant depth back into the underlying metamorphic rocks (Fig. 10). If the fault fluids were re-mixing with fluids from the underlying metamorphic rocks, we would expect to see progressively lower salinities with increasing distance from the fault, producing a plot with a linear trend instead of showing an abrupt decrease at 50 m. The silica-rich fluids rising from the footwall do not seem to penetrate the Tuscan nappe above the fault zone either, since no quartz veins, which are common in the metamorphic rocks, are found above the fault, only calcite veins.

It is unclear whether fluids that have been trapped within the Alpi Apuane fault zone came from one or more sources. Since the fault zone contains quartz veins but no quartz veins are seen in the Tuscan nappe above, it is likely that the silica-rich fluids in the fault zone

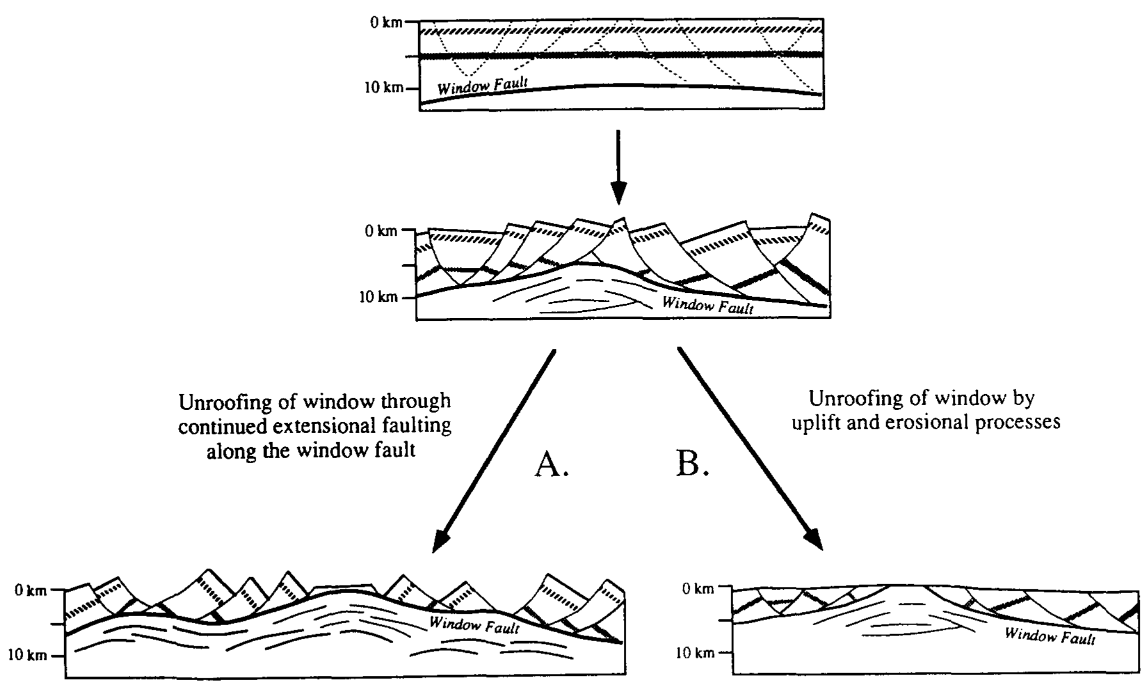

Fig. 8. Two possible scenarios for the structural evolution of the Alpi Apuane window. Model 'A' shows total unroofing of the window by extension along the window fault. In this case, extensional motion on the window fault occurs initially at mid-crustal levels (8–10 km) and remains active as the footwall rocks are brought to shallower and shallower levels. In model 'B', extensional motion on the window fault only occurs at mid-crustal levels (8–10 km). Final unroofing of the rocks inside the window is accomplished through uplift and erosion with no further motion on the window fault.

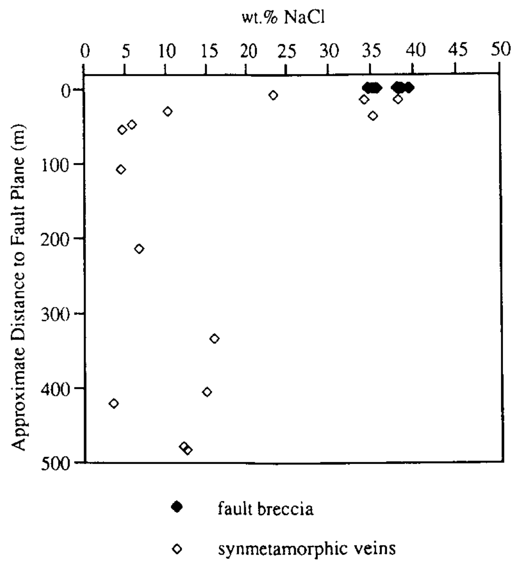

Fig. 9. Salinities of fluids in the fault breccia and synmetamorphic veins of the footwall vs distance from the fault zone. The plot excludes samples R-2, MA-1 and MA-6 due to inadequate estimates for distance to the fault plane. Salinities are presented as sample averages.

originated as metamorphic fluids in the footwall below. These fluids then rose into the fault zone and were channeled within it.

Acknowledgements—Financial support for this project was provided by a Martin Fellowship from the University of North Carolina at Chapel Hill, an Amoco Geophysical Fellowship, grants from the Sigma Xi Foundation and the Geological Society of America, and the Frederick A. Sutton Grant and the Marta S. Weeks Grant from the American Association of Petroleum Geologists, all awarded to Margaret Hodgkins. Additional support was provided by a University of North Carolina University Research Council grant and Junior Faculty Development grant awarded to Kevin Stewart. We thank David Bice and Steven Lundblad for helpful discussions and assistance in the field; Robert Bodnar for helping us analyze and understand our fluid inclusion data, and also for the use of his laboratory at VPI; Geoff Feiss for his helpful comments and use of his fluid inclusion analysis system; Anne-Marie Boullier, Kieran O'Hara, Karen Carter and an anonymous reviewer for their thorough reviews of the manuscript; and James Evans, John J. W. Rogers, Roy Kligfield, Luigi Carmignani and Michael Follo for helpful reviews of earlier versions of the manuscript.

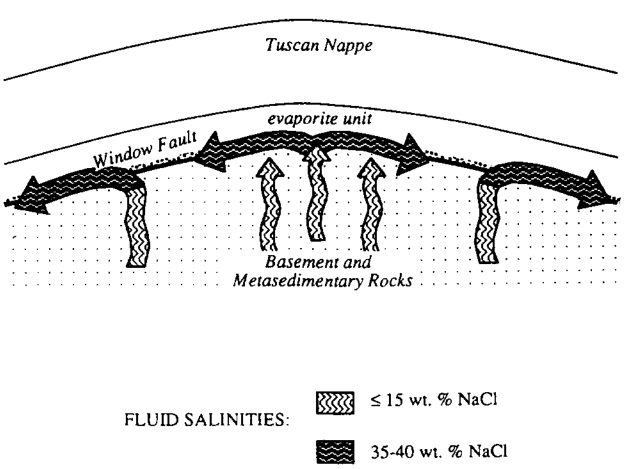

Fig. 10. Schematic diagram for fluid flow within the Alpi Apuane. Fluids rising from the footwall are of moderate salinities (≤15 wt% NaCl). Once the fluids enter the fault zone, they are channeled within it, leach salt from the evaporite unit above, and become saturated with NaCl (35–40 wt% NaCl). Based on the pattern of salinities, it does not appear that the fluids entering the fault zone re-circulate into the footwall.

REFERENCES

Abbate, E. & Bruni, P. 1989. Torbiditi oligo-mioceniche ed evoluzione del margine Nord-Appenninico. *Mem. Soc. geol. Ital.* **39**, 19–33.

Abbate, E. & Sagri, M. 1970. Development of the Northern Apennines geosyncline: The eugeosynclinal sequences. *Sediment. Geol.* **4**, 251–340.

Alvarez, W. 1991. Tectonic evolution of the Corsica–Appenines–Alps region studied by the method of successive approximations. *Tectonics* **10**, 936–947.

Baldacci, F., Elter, P., Giannini, E., Giglia, G., Lazzarotto, A., Nardi, R. & Tongiorgi, M. 1967. Nuove osservazioni sul problema della falda toscana e sulla interpretazione dei flysch arenacei tipo "Macigno" del'Appennino settentrionale. *Mem. Soc. geol. Ital.* **6**, 199–211.

Bally, A. W., Burbi, L., Cooper, C. & Ghelardoni, R. 1986. Balanced sections and seismic reflection profiles across the central Apennines. *Mem. Soc. geol. Ital.* **35**, 257–310.

Boccaletti, M. & Guazzone, G. 1968. A contribution to the regional study of structural–stratigraphic units by systematic analysis of structural trends, 1. Serie toscana. *Mem. Soc. geol. Ital.* **7**, 247–260.

Bodnar, R. J. 1983. A method of calculating fluid inclusion volumes based on vapor bubble diameters and *P–V–T–X* properties of inclusion fluids. *Econ. Geol.* **78**, 535–542.

Bodnar, R. J. & Sterner, S. M. 1985. Synthetic fluid inclusions in natural quartz. II. Application to PVT studies. *Geochim. cosmochim. Acta* **49**, 1855–1859.

Bodnar, R. J., Sterner, S. M. & Hall, D. L. 1989. Salty: A Fortran program to calculate compositions of fluid inclusions in the system NaCl–KCl–H_2O. *Comput. & Geosci.* **15**, 19–41.

Bortolotti, V., Passerini, P., Sagri, M. & Sestini, S. 1970. Development of the Northern Apennines geosyncline: The miogeosynclinal sequences. *Sediment. Geol.* **4**, 341–444.

Boullier, A.-M., France-Lanord, C., Dubessy, J., Adamy, J. & Champenois, M. 1991. Linked fluid and tectonic evolution in the High Himalaya mountains (Nepal). *Contr. Miner. Petrol.* **107**, 358–372.

Bozzo, A. T., Chen, H.-S., Kass, J. R. & Barduhn, A. J. 1975. The properties of the hydrates of chlorine and carbon dioxide. *Desalination* **16**, 303–320.

Brown, P. E. 1989. FLINCOR: A fluid inclusion data reduction and exploration program. *Second Biennial Pan-American Conf. on Research on Fluid Inclusions Prog. with Abs.* **14**.

Brown, P. E. & Lamb, W. M. 1989. P–V–T properties of fluids in the system H_2O–CO_2–NaCl: New graphical presentations and implications for fluid inclusion studies. *Geochim. cosmochim. Acta* **45**, 1209–1221.

Carmignani, L. & Giglia, G. 1975. Le fasi tettoniche terziare dell'autoctono delle Alpi Apuane: Studio delle strutture minori della zona centro-meridionale. *Boll. Soc. geol. Ital.* **94**, 1957–1981.

Carmignani, L. & Giglia, G. 1977. Analasi mesostrutturale della zona occidentale delle Apuane metamorfiche. *Boll. Soc. geol. Ital.* **96**, 429–450.

Carmignani, L. & Giglia, G. 1983. Il problema della doppia vergenza sulle Alpi Apuane e la struttura del M. Corchia. *Mem. Soc. geol. Ital.* **26**, 515–525.

Carmignani, L., Giglia, G. & Kligfield, R. 1978. Structural evolution of the Apuane Alps: An example of continental margin deformation in the Northern Apennines. Italy. *J. Geol.* **86**, 487–504.

Carmignani, L. & Kligfield, R. 1990. Crustal extension in the Northern Apennines: The transition from compression to extension in the Alpi Apuane core complex. *Tectonics* **9**, 1275–1303.

Cathelineau, M., Lespinasse, M., Bastoul, A. M., Bernard, C. & Leroy, J. 1990. Fluid migration during contact metamorphism: The use of oriented fluid inclusion trails for a time/space reconstruction. *Mineralog. Mag.* **54**, 169–182.

Cerrina Feroni, A., Nuti, S., Pertusati, P. C. & Plesi, G. 1976. Sulla probabile origine carsica delle brecce sedimentarie associate al calcare cavernoso dell'Appennino settentrionale. *Boll. Soc. geol. Ital.* **95**, 1161–1174.

Cerrina Feroni, A., Plesi, G., Leoni, L. & Martinelli, P. 1983. Contributo alla conoscenza dei processi metamorfici di grado molto basso (anchimetamorfismo) a carico della falda toscana nell'area di riccoprimento apuano. *Boll. Soc. geol. Ital.* **102**, 269–280.

Dallan Nardi, L. 1979. Microfossili miocenici nella matrice sedimentaria delle brecce situate alla base della "Falda Toscana" nelle Apuane meridionali. *Boll. Soc. geol. Ital.* **98**, 119–128.

Dallan Nardi, L. & Nardi, R. 1973. Ipotesi sulla genesi e sul significato delle brecce stratigrafiche associate ai "calcare cavernosi" sulle Alpi Apuane e sul Monte Pisano in rapporto alla messa in posto della falda toscana. *Boll. Soc. geol. Ital.* **92**, 435–452.

de Alvarenga, C. J. S., Cathelineau, M. & Dubessy, J. 1990. Chronology and orientation of N_2–CH_4, CO_2–H_2O-rich fluid-inclusion trails in intrametamorphic quartz veins from the Cuiabà gold district, Brazil. *Mineralog. Mag.* **54**, 245–255.

DiPisa, A., Franceschelli, M., Leoni, L. & Meccheri, M. 1985. Regional variation of the metamorphic temperatures across the Tuscanid I Unit and its implications on the alpine metamorphism (Apuan Alps, N. Tuscany). *Neues Jb. Mineral. Abh.* **51**, 197–211.

Elter, P., Giglia, G., Tongiorgi, M. & Trevisan, L. 1975. Tensional and compressional areas in the recent (Tortonian to present) evolution of the Northern Apennines. *Boll. Geofis. Teor. Appl.* **42**, 3–18.

Etheridge, M. A., Wall, V. J. & Vernon, R. H. 1983. The role of the fluid phase during regional metamorphism and deformation. *J. metamorph. Geol.* **1**, 205–226.

Federici, P. & Raggi, G. 1974. Brecce sedimentarie e rapporti tra le unita' tettoniche toscane nel gruppo delle Alpi Apuane. *Boll. Soc. geol. Ital.* **93**, 709–722.

Foreman, J. L. & Dunne, W. M. 1991. Conditions of vein formation in the southern Appalachian foreland: constraints from vein geometries and fluid inclusions. *J. Struct. Geol.* **13**, 1173–1183.

Franceschelli, M., Leoni, L., Memmi, I. & Puxeddu, M. 1986. Regional distribution of Al-silicates and metamorphic zonation in the low-grade Verrucano metasediments from the Northern Apennines, Italy. *J. metamorph. Geol.* **4**, 309–321.

Fyfe, W. S. & Kerrich, R. 1985. Fluids and thrusting. *Chem. Geol.* **49**, 353–362.

Giglia, G. 1967. Geologia dell'alta Versilia settentrionale (tav. M. Altissimo). *Mem. Soc. geol. Ital.* **6**, 67–96.

Haas, J. L. 1976. Physical properties of the coexisting phases and thermochemical properties of the H_2O component in boiling NaCl solutions. *Bull. U.S. geol. Surv.* **1421-A**.

Hall, D. L., Sterner, S. M. & Bodnar, R. J. 1988. Freezing point depression of NaCl–KCl–H_2O solutions. *Econ. Geol.* **83**, 197–202.

Hendel, E. M. & Hollister, L. S. 1981. An empirical solvus for CO_2–H_2O–2.6 wt% salt. *Geochim. cosmochim. Acta* **45**, 225–228.

Hollister, L. S. 1981. Information intrinsically available from fluid inclusions. In: *Short Course in Fluid Inclusions* (edited by Hollister, L. S. & Crawford, M. L.). Mineralogical Association of Canada, Calgary, 1–12.

Hubbert, M. K. & Rubey, W. W. 1959. Role of fluid pressure in mechanics of over-thrust faulting. *Bull. geol. Soc. Am.* **70**, 115–166.

Kligfield, R. 1979. The Northern Apennines as a collisional orogen. *Am. J. Sci.* **279**, 676–691.

Kligfield, R., Carmignani, L. & Owens, W. 1981. Strain analysis of a Northern Apennines shear zone using deformed marble breccias. *J. Struct. Geol.* **3**, 421–436.

Kligfield, R., Hunziker, J., Dallmeyer, R. D. & Schamel, S. 1986. Dating of deformation phases using K-Ar and 40Ar/39Ar techniques: Results from the Northern Apennines. *J. Struct. Geol.* **8**, 781–798.

Malinverno, A. & Ryan, W. 1986. Extension in the Tyrrhenian Sea and shortening in the Apennines as result of arc migration driven by sinking of the lithosphere. *Tectonics* **5**, 227–246.

Oliver, J. 1986. Fluids expelled tectonically from orogenic belts: Their role in hydrocarbon migration and other geologic phenomena. *Geology* **14**, 99–102.

Parry, W. T. & Bruhn, R. L. 1987. Fluid inclusion evidence for minimum 11 km vertical offset on the Wasatch fault, Utah. *Geology* **15**, 67–70.

Reutter, K., Teichmuller, M., Teichmuller, R. & Zanzucchi, G. 1980. Le ricerche sulla carbonificazione dei frustoli vegetali nelle rocce clastiche come contributo ai problemi di paleogeotermia e tettonica nell'Appennino settentrionale. *Mem. Soc. geol. Ital.* **21**, 111–116.

Reutter, K., Teichmuller, M., Teichmuller, R. & Zanzucchi, G. 1983. The coalification pattern in the Northern Apennines and its Palaeogeothermic and tectonic significance. *Geol. Rdsch.* **72**, 861–894.

Roedder, E. 1984. *Fluid Inclusions*, Bookcrafters, Chelsea, Michigan.

Roedder, E. & Bodnar, R. J. 1980. Geologic pressure determinations from fluid inclusion studies. *Annu. Rev. Earth & Planet. Sci.* **8**, 263–301.

Saggini, F. 1965. Per una rinnovata interpretazione regionale dei "raddoppi" tettonici locali della serie toscana. *Boll. Soc. geol. Ital.* **84**, 311–344.

Sani, M. 1985. Le brecce della Versilia tra successione Toscana metamorfica e Falda Toscana nell'area di Casoli-Metato (Apuane meridionali). *Rend. Soc. Geol. Ital.* **8**, 25–29.

Sterner, S. M. & Bodnar, R. J. 1989. Synthetic fluid inclusions—VII. Re-equilibration of fluid inclusions in quartz during laboratory-simulated metamorphic burial and uplift. *J. metamorph. Geol.* **7**, 243–260.

Srivastava, D. C. & Engelder, T. 1991. Fluid evolution history of brittle-ductile shear zones in the hanging wall of Yellow Spring thrust, Valley and Ridge Province, Pennsylvania, U.S.A. *Tectonophysics* **198**, 23–34.

Touret, J. 1977. The significance of fluid inclusions in metamorphic rocks. In: *Thermodynamics in Geology* (edited by Fraser, D. G.). D. Reidel, Boston, 203–227.

Treves, B. 1984. Orogenic belts as accretionary prisms: The example of the Northern Apennines. *Ofioliti* **9**, 577–618.

Van den Berg, L. 1990. Application of a mechanical model to the Northern Apennines, with special reference to the effect of sea level changes. *Geologie Mijnb.* **69**, 43–52.

Venturelli, G. & Frey, M. 1977. Anchizone metamorphism in sedimentary sequences of the Northern Apennines. *Rend. Soc. Ital. Miner. Petrol.* **33**, 109–123.

Vrolijk, P. 1987. Tectonically driven fluid flow in the Kodiak accretionary complex, Alaska. *Geology* **15**, 466–469.

Yonkee, W. A., Parry, W. T., Bruhn, R. L., & Cashman, P. H. 1989. Thermal models of thrust faulting: Constraints from fluid-inclusion observations, Willard thrust sheet, Idaho–Utah–Wyoming thrust belt. *Bull. geol. Soc. Am.* **101**, 304–313.